Herceptin induces ferroptosis and mitochondrial dysfunction in H9c2 cells

LEI SUN, HUA WANG, SHANSHAN YU, LIN ZHANG, JUE JIANG and QI ZHOU

Department of Ultrasound, The Second Affiliated Hospital of Xi'an Jiaotong University, Xi'an, Shaanxi 710004, P.R. China

Received May 16, 2021; Accepted September 10, 2021

DOI: 10.3892/ijmm.2021.5072

Abstract. Ferroptosis has been previously implicated in the pathological progression of cardiomyopathy. Herceptin (trastuzumab), which targets HER2, is commonly applied for the treatment of $HER2^+$ breast cancer. However, its clinical use is limited by its cardiotoxicity. Therefore, the present study aimed to investigate if targeting ferroptosis could protect against Herceptin-induced heart failure in an *in vitro* model of H9c2 cells after treatment of Herceptin, Herceptin + ferroptosis inhibitor ferrostatin-1 (Fer-1) or Herceptin + Deferoxamine. H9c2 cell viability was measured by MTT assay. Reactive oxygen species (ROS) levels were detected by measuring the fluorescence of DCFH-DA-A and MitoSOX™ Red. Glutathione (GSH)/oxidized glutathione (GSSG) ratio was measured using the GSH/GSSG Ratio Detection Assay kit. Mitochondrial membrane potential and ATP content were evaluated by JC-1 staining and bioluminescent assay kits, respectively. Protein expressions of glutathione peroxidase 4, recombinant solute carrier family 7 member 11, mitochondrial optic atrophy1-1/2, mitofusin, Acyl-CoA synthetase long chain family member 4, cytochrome *c*, voltage-dependent anion-selective channel, dynamin-related protein, mitochondrial fission 1 protein and mitochondrial ferritin were evaluated by western blotting. It was found that Herceptin reduced H9c2 cell viability whilst increasing intracellular and mitochondrial ROS levels in a dose- and time-dependent manner. Furthermore, Herceptin decreased glutathione peroxidase (GPX) protein expression and the GSH/GSSG ratio in H9c2 cells in a dose- and time-dependent manner. The Fer-1 abolished this Herceptin-induced reduction in cell viability, GSH/GSSG ratio, mitochondrial membrane potential and ATP content. Fer-1 also reversed the suppressive effects of Herceptin on the protein expression levels of GPX4, recombinant solute carrier family 7 member 11, mitochondrial optic atrophy1-1/2 and mitofusin in H9c2 cells. Subsequently, Fer-1 was found to reverse the Herceptin-induced increase in mitochondrial ROS and iron levels in H9c2 cells, as well as the increased protein expression levels of Acyl-CoA synthetase long chain family member 4, cytochrome *c*, voltage-dependent anion-selective channel, dynamin-related protein, mitochondrial fission 1 protein and mitochondrial ferritin in H9c2 cells. However, compared with deferoxamine, an iron chelator, the effects of Fer-1 were less effective. Collectively, these findings provided insights into the pathogenic mechanism that underlie Herceptin-induced cardiomyopathy, which potentially provides a novel therapeutic target for the prevention of cardiotoxicity in $HER2^+$ breast cancer treatment.

Introduction

Cell death is an essential physiological process that is key in tissue homeostasis, aging, development and various pathological states (1). Ferroptosis is a newly identified type of cell death that is characterized by the iron-dependent accumulation of lipid peroxides to lethal levels, which is genetically, biochemically and morphologically distinct from autophagy, necroptosis and apoptosis (2). Ferroptosis can be prevented or reversed by iron chelation (3) and has been previously shown to be involved in the pathological progression of carcinogenesis (4), renal ischemia/reperfusion injury (5) and oxidative stress-induced cell death (6).

Herceptin (trastuzumab) is a chemotherapeutic agent that targets HER2 and is commonly utilized for the treatment of patients with $HER2^+$ breast cancer (7). However, the clinical use of Herceptin is limited due to its reported cardiotoxic effects, including congestive heart failure and irreversible degenerative cardiomyopathy (8-10). Death of terminally differentiated cardiomyocytes is one of the major pathogenic causes of heart injury (11). Therefore, preventing cardiomyocyte cell death is proposed to be an effective cardioprotective approach (11).

Iron homeostasis is sustained by several mechanisms, including hepcidin and iron regulatory proteins (IRP), including IRP1 and IRP2, at systemic and cellular levels (12). Disruption of iron homeostasis leads to excessive intracellular iron accumulation, thereby causing the oxidation and modification of lipids, proteins and DNA through the production of free radicals and oxidative stress (13). Aberrant dysregulation of iron metabolism is associated with in a number diseases, including

Correspondence to: Dr Qi Zhou, Department of Ultrasound, The Second Affiliated Hospital of Xi'an Jiaotong University, 157 Xiwu Road, Xi'an, Shaanxi 710004, P.R. China
E-mail: zhouqixajtu@tom.com

Key words: Herceptin, cardiotoxicity, ferroptosis, mitochondrial dysfunction

neurodegenerative diseases (Alzheimer's disease, Parkinson's disease and Huntington's disease) (14,15), cancer (lung cancer, colon cancer and breast cancer) (16,17) and cardiovascular diseases (atherosclerosis and myocardial ischemia-reperfusion injury) (18,19). Dysregulation of iron homeostasis results in excessive iron deposition in several organs, leading to progressive tissue damage (20). Iron overload serves a pathogenic role in cardiomyopathy by generating ROS via the Fenton reaction and exerts harmful influences (18,21). In 2012, iron-dependent cell death (ferroptosis) was discovered for the first time by Dixon *et al* (2). In animal models of cardiomyopathy and patients with heart failure, iron overload has been revealed to mediate the pathogenesis of cardiotoxicity under numerous cardiopathic conditions, where doxorubicin toxicity typically occurs by the preferential accumulation of iron specifically in the mitochondria independent of the topoisomerase-2β (a well-known target of doxorubicin) pathway (22,23). However, little is known regarding the underlying mechanism of iron accumulation or its toxicity. The present study therefore aimed to investigate the effects of targeting ferroptosis on Herceptin-induced heart failure in an *in vitro* model.

Materials and methods

Cell culture and in vitro treatment. H9c2 rat cardiomyocytes were purchased from The Cell Bank of Type Culture Collection of The Chinese Academy of Sciences. Cells were incubated in DMEM (Gibco; Thermo Fisher Scientific, Inc.) containing 10% heat-inactivated FBS (Gibco; Thermo Fisher Scientific, Inc.) and 1% penicillin-streptomycin (Gibco; Thermo Fisher Scientific, Inc.) at 37˚C in a humidified atmosphere containing 5% CO_2.

Herceptin [0, 0.2, 0.5, 1 and 10 μM; Genentech Inc.; Roche Pharma (Schweiz) Ltd.] was administrated for 12, 24 or 48 h at 37˚C (24). The ferroptosis inhibitor, ferrostatin-1 (Fer-1; Sigma-Aldrich; Merck KGaA), a lipid reactive oxygen species (ROS) scavenger, was initially dissolved in DMSO and diluted to a final concentration of 10 μM (25). Deferoxamine (DFO; cat. no. HY-B0988; MedChem Express), which is an iron chelator, was diluted to a final concentration of 100 μM (26). H9c2 rat cardiomyocytes were randomly divided into the following four groups: i) Control; ii) Herceptin; iii) Herceptin + Fer-1; and iv) Herceptin + DFO. Fer-1 or DFO was co-administrated with Herceptin. Samples were collected at the indicated time points after Herceptin treatment.

Cell viability. Cell viability was assessed using MTT assay. Briefly, H9c2 cells ($3x10^4$ cells/well) were seeded into 96-well plates and incubated at 37˚C for 24 h. Following the aforementioned treatments, H9c2 cells were added with a MTT solution (5 mg/ml) and incubated for 4 h at 37˚C. Next, DMSO was added into each well to lyse the cells and dissolve the formazan crystals after the removal of supernatant. The absorbance at 570 nm was recorded in each well with a Flexstation® 3 microplate reader (Molecular Devices, LLC). The optical density value was reported as the ratio to control group (set as 100%).

Measurement of intracellular and mitochondrial ROS. The intracellular and mitochondrial ROS levels were quantified by measuring the fluorescence of DCFH-DA-A (cat. no. S0033; Beyotime Institute of Biotechnology) and MitoSOX™ Red (Mitochondrial Superoxide Indicator; cat. no. M36008; Thermo Fisher Scientific, Inc.), respectively. After the aforementioned treatments, H9c2 cells were collected and washed three times with 1X PBS, followed by incubation with 5 μM DCFH-DA-A or MitoSOX™ Red for 45 min at 37˚C in the dark. H9c2 cells were then washed three times with 1X PBS and detached with trypsin/EDTA. The relative level of cellular fluorescence was quantified by flow cytometry (BD FACSCanto™; BD Biosciences). Data were analyzed using FlowJo version x0.7 (FlowJo LLC).

Measurement of glutathione (GSH)/oxidized glutathione (GSSG) ratio. H9c2 cells ($5x10^4$ cells/well) were seeded into 96-well white-walled multiwall luminometer plates. After treatment with Herceptin (0, 0.2, 0.5, 1 and 10 μM) for 12, 24 and 48 h at 37˚C, the GSH/GSSG ratio was detected using a GSH/GSSG Ratio Detection Assay kit (cat. no. ab138881; Abcam), following the manufacturer's protocols.

Western blot analysis. Total protein was extracted from H9c2 cells via homogenization in RIPA buffer (cat. no. P0013B; Beyotime Institute of Biotechnology) containing protease inhibitors. Protein concentration was evaluated using a Pierce BCA protein assay kit (Thermo Fisher Scientific, Inc.). In total, 20 μg protein was separated by 10-12% SDS-PAGE and subsequently transferred onto nitrocellulose membranes. The membranes were blocked with 5% BSA (Thermo Fisher Scientific, Inc.) in TBS containing 0.2% Tween-20 for 1 h, followed by an overnight incubation at 4˚C with primary antibodies against glutathione peroxidase (GPX)4 (cat. no. DF6701; dilution 1:1,000; Affinity Biosciences), recombinant solute carrier family 7 member 11 (SLC7A11; cat. no. A13685; dilution 1:1,000; ABclonal Biotech Co., Ltd.), acyl-CoA synthetase long chain family member 4 (ACSL4; cat. no. DF12141; dilution 1:1,000; Affinity Biosciences), voltage-dependent anion-selective channel (VDAC2/3; cat. nos. 11663-1-AP and 14451-1-AP; dilution 1:1,000; Proteintech Group, Inc.), cytochrome *c* (Cyto *c*; cat. no. 10993-1-AP; dilution 1:1,000; Proteintech Group, Inc.), mitochondrial fission 1 protein (fis1; cat. no. 10956-1-AP; dilution 1:1,000; Proteintech Group, Inc.), mitofusin (Mfn1/2; cat. no. 13798-4-AP; dilution 1:1,000; Proteintech Group, Inc.), dynamin-related protein (Drp1; cat. no. ab184247; dilution 1:1,000; Abcam), mitochondrial optic atrophy (OPA1-1/2; cat. no. 27733-1-AP; dilution 1:2,000; Proteintech Group, Inc.), mitochondrial ferritin (Mtf; cat. no. LS0-C293861; dilution 1:500; Lifespan BioSciences, Inc.) and GAPDH (cat. no. AB-P-R001; dilution 1:1,000; Hangzhou Xianzhi Biological Technology Co., Ltd.). The membranes were then incubated for 1 h at room temperature with an HRP-conjugated secondary antibody (cat. no. BA1054; dilution 1:5,000; Boster Biological Technology). Finally, the bands were detected using the Pierce ECL system (Thermo Fisher Scientific, Inc.) and band intensity quantified using the ImageJ software (version 1.8.0; National Institutes of Health).

Measurement of intracellular labile iron pool (LIP). H9c2 cells ($1x10^4$ cells/well) were seeded into a 96-well plate and grown overnight. The H9c2 cells were then harvested, washed and resuspended in a buffer containing 140 mM NaCl, 5 mM KCl, 1 mM $MgCl_2$, 5.6 mM glucose, 1.5 mM

$CaCl_2$ and 20 mM HEPES (pH 7.4), followed by the addition of 0.25 mM Calcein-AM (cat. no. C2012; Beyotime Institute of Biotechnology). This reaction mixture was incubated for 30 min at 37˚C and washed three times with the buffer aforementioned prior to the resuspension of H9c2 cells. The fluorescence intensity of Calcein-AM was quantified using a microplate reader (Synergy H4; 488 nm excitation and 525 nm emission; BioTek China). After the baseline became stable, salicylaldehyde isonicotinoyl hydrazone (SIH, 100 μM) which was synthetized by Schiff base condensation between 2-hydroxybenzaldehyde and isonicotinic acid hydrazide (Shanghai Nafu Biotechnology Co., Ltd.; https://nayuansu.company.lookchem.cn/) was added. The reaction mixture was subsequently incubated for 30 min at 37˚C before the fluorescence intensity was detected. Calcein-AM itself has no fluorescence. After entering the H9c2 cells, it is hydrolyzed by endogenous esterase in the H9c2 cells to produce Calcein, a polar molecule with strong negative charge that cannot penetrate the cell membrane, which is retained in the cell and emit strong green fluorescence. The increase in fluorescence intensity indicates the level of Calcein-bound iron. The results were presented as fluorescence intensity/mg protein.

Measurement of mitochondrial iron. Mitochondria were isolated from H9c2 cells ($1x10^6$ cells/dish) using a Mitochondria Isolation kit for Cultured Cells (Thermo Fisher Scientific, Inc.) according to the manufacturer's protocol. The levels of iron in the mitochondria was then determined using an Iron Colorimetric assay kit (cat. no. BIV-K390-100; BioVision, Inc.) according to the manufacturer's protocol. The absorbance was measured at 593 nm using a TECAN infinite M200 microplate reader (Tecan Group, Ltd.).

5,5',6,6'-Tetrachloro-1,1',3,3'-tetraethylbenzimidazolocarbocyanine iodide (JC-1) staining. Following JC-1 staining (cat. no. C2006; Beyotime Institute of Biotechnology) at 37˚C for 10 min, H9c2 cells ($5x10^4$/well) were washed with the JC-1 staining buffer three times and detected via flow cytometry (BD FACSCanto™; BD Biosciences). Data were analyzed using FlowJo version x0.7 (FlowJo LLC). In the healthy mitochondria, JC-1 aggregated to form a polymer in the mitochondrial matrix, which emits intense red fluorescence (Excitation, 585 nm; Emission, 590 nm). In the unhealthy mitochondria, JC-1 monomers presented in the cytoplasm due to the decline/loss of mitochondrial membrane potential, which generate green fluorescence (Excitation, 514 nm; Emission, 529 nm). Therefore, changes in ratio of H1-UL (red)/H1-UR (green) reflected the change in mitochondrial membrane potential.

ATP content. H9c2 cells ($1x10^4$ cells/well) were lysed by ATP lysis buffer on ice, exposed to the ATP substrate solution and cellular ATP content was determined by bioluminescent assay kit (cat. no. ab113849; Abcam).

Statistical analysis. Data were repeated ≥ three times independently, analyzed using GraphPad Prism software (version 6.01, GraphPad Software, Inc.) and are presented as the mean ± SD. Groups were compared using one-way ANOVA followed by Tukey's post hoc test. $P<0.05$ was considered to indicate a statistically significant difference.

Results

Herceptin induces cell injury and oxidative stress in H9c2 cells. Herceptin (0, 0.2, 0.5, 1 and 10 μM) was found to reduce H9c2 cell viability in a dose-dependent manner (Fig. 1A). In addition, 10 μM Herceptin reduced H9c2 cell viability in a time-dependent manner from 12 to 48 h (Fig. 1B). Herceptin (0, 0.2, 0.5, 1 and 10 μM) also dose-dependently increased intracellular (Fig. 1C) and mitochondrial (Fig. 1E) ROS levels in H9c2 cells. Furthermore, Herceptin (10 μM) increased intracellular (Fig. 1D) and mitochondrial (Fig. 1F) ROS levels in H9c2 cells from 12 to 48 h, peaking at 24 h.

Herceptin induces ferroptosis in H9c2 cells. Herceptin (0, 0.2, 0.5, 1 and 10 μM) dose-dependently reduced the protein expression of GPX4 in H9c2 cells (Fig. 2A), whilst at 10 μM Herceptin also inhibited GPX4 protein expression in H9c2 cells in a time-dependent manner from 12 to 48 h (Fig. 2B). Herceptin (0, 0.2, 0.5, 1 and 10 μM) decreased GSH content (Fig. 2C) and increased the GSSG content (Fig. 2D), thereby decreasing the GSH/GSSG ratio in H9c2 cells in a dose-dependent manner (Fig. 2E). Furthermore, Herceptin at 10 μM decreased the GSH content (Fig. 2F) whilst increasing that of GSSG (Fig. 2G), which resulted in the reduction in the GSH/GSSG ratio in H9c2 cells in a time-dependent manner from 12 to 48 h (Fig. 2H).

Fer-1 protects H9c2 cells against Herceptin-induced cell injury and ferroptosis. Fer-1 treatment was found to reverse the Herceptin-induced reduction in cell viability (Fig. 3A), restored GPX4 and SLC7A11 expression that was previously suppressed by Herceptin whilst reversing the Herceptin-induced increase in ACSL14 expression (Fig. 3B). Fer-1 was also revealed to partially restore GSH production that was previously suppressed by Herceptin without affecting the GSSG content, which in turn lead to the reversal of the Herceptin-induced reduction in GSH/GSSG ratio in H9c2 cells (Fig. 3C-E). Additionally, Fer-1 reversed the Herceptin-induced increase in intracellular (Fig. 3F) and mitochondrial (Fig. 3G) iron levels in H9c2 cells. However, compared with those mediated by DFO, the effects of Fer-1 were less potent.

Fer-1 protects H9c2 cells from Herceptin-induced mitochondrial dysfunction. Fer-1 was demonstrated to reverse the Herceptin-induced reduction in ATP production (Fig. 4A). In addition, Fer-1 could negate the Herceptin-mediated increases in mitochondrial ROS production (Fig. 4B) whilst reversing the Herceptin-induced decrease in mitochondrial membrane potential (Fig. 4C). In terms of protein expression, Herceptin increased Cyto *c*, VDAC2/3, fis1, Drp1 and Mtf protein expression but decreased OPA1-1/2 and Mfn1/2 expression (Fig. 4D), all of which were reversed by Fer-1 co-treatment. However, compared with DFO, the effects mediated by Fer-1 were not as potent.

Discussion

The present study discovered that Herceptin induced injury, oxidative stress, mitochondrial dysfunction and ferroptosis in H9c2 cells, which could be attenuated by Fer-1. Oxidative

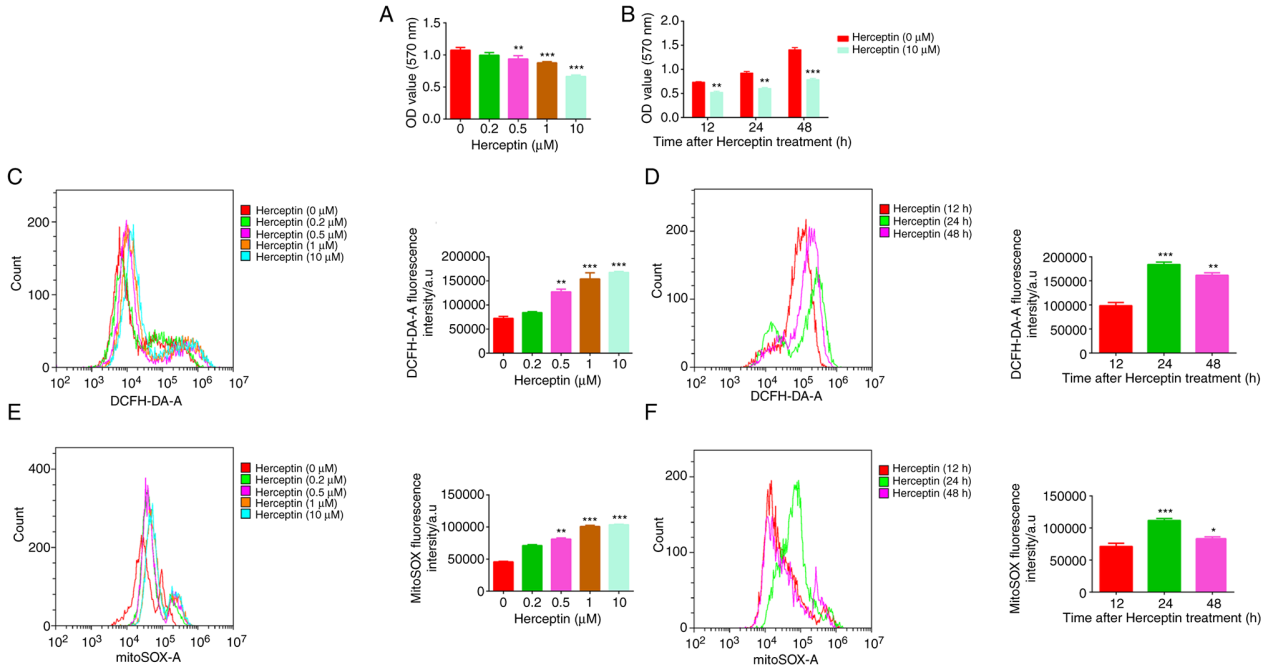

Figure 1. Herceptin induces cell injury and oxidative stress in H9c2 cells. Herceptin decreased H9c2 cell viability in a (A) dose- and (B) time-dependent manner. (C) Herceptin increased ROS levels in H9c2 cells in a dose-dependent manner. (D) Herceptin increased ROS production in H9c2 cells from 12 to 48 h, peaking at 24 h. (E) Herceptin increased ROS levels in mitochondria in a dose-dependent manner. (F) Herceptin increased ROS levels in mitochondria from 12 to 48 h, peaking at 24 h. *P<0.05, **P<0.01 and ***P<0.001 vs. 0 μM or 12 h. ROS, reactive oxygen species.

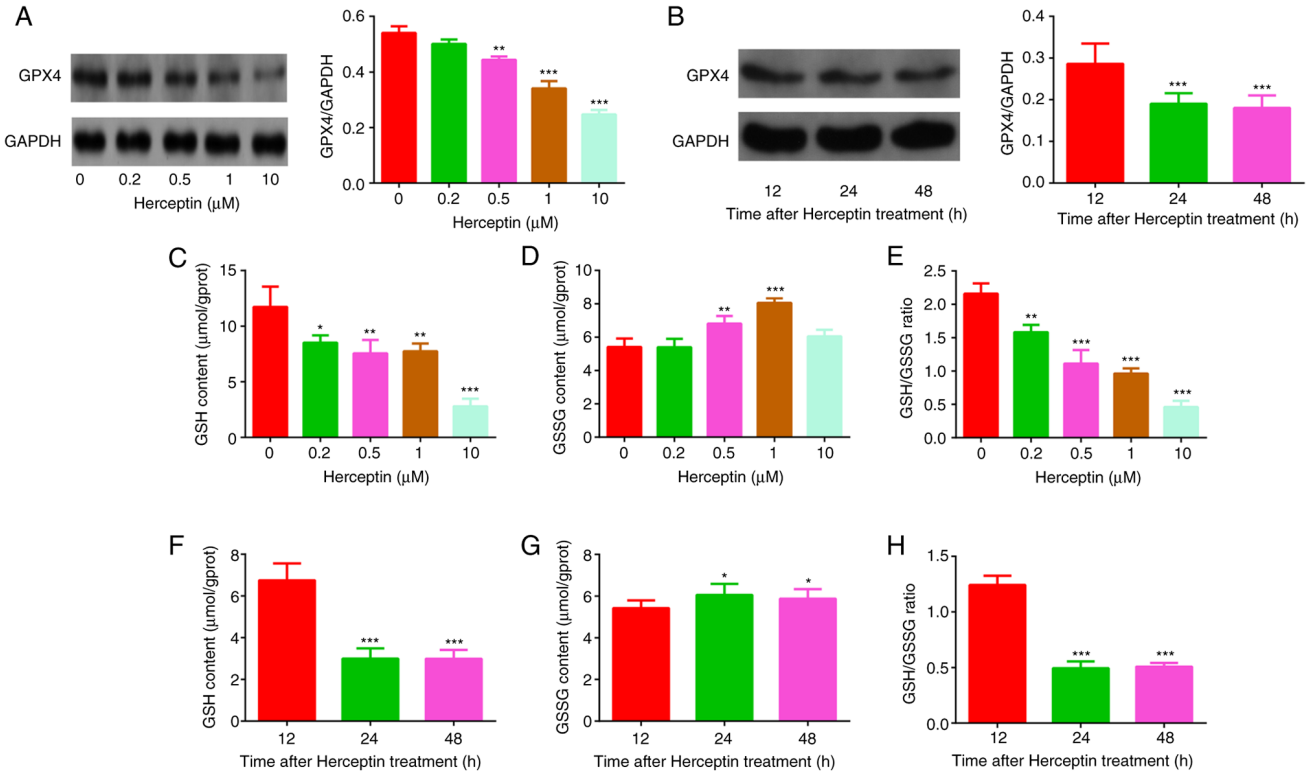

Figure 2. Herceptin induces ferroptosis in H9c2 cells. Herceptin reduced GPX4 protein expression in a (A) dose-dependent and (B) time-dependent manner. Herceptin (C) decreased GSH content whilst (D) increasing GSSG content, (E) consequently reducing the GSH/GSSG ratio, in H9c2 cells in a dose-dependent manner. Herceptin (F) decreased GSH content whilst (G) increasing GSSG content, (H) consequently reducing the GSH/GSSG ratio, in H9c2 cells. *P<0.05, **P<0.01 and ***P<0.001 vs. 0 μM or 12 h. GPX, glutathione peroxidase; GSH, reduced glutathione; GSSG, oxidized glutathione.

stress has been frequently reported to mediate cellular and molecular damage resulting from excessive ROS production caused by the inhibition of antioxidant enzyme systems and/or insufficient antioxidants production (27). This can cause numerous diseases, including cardiovascular diseases (27). The overproduction of ROS leads to the dysregulation of

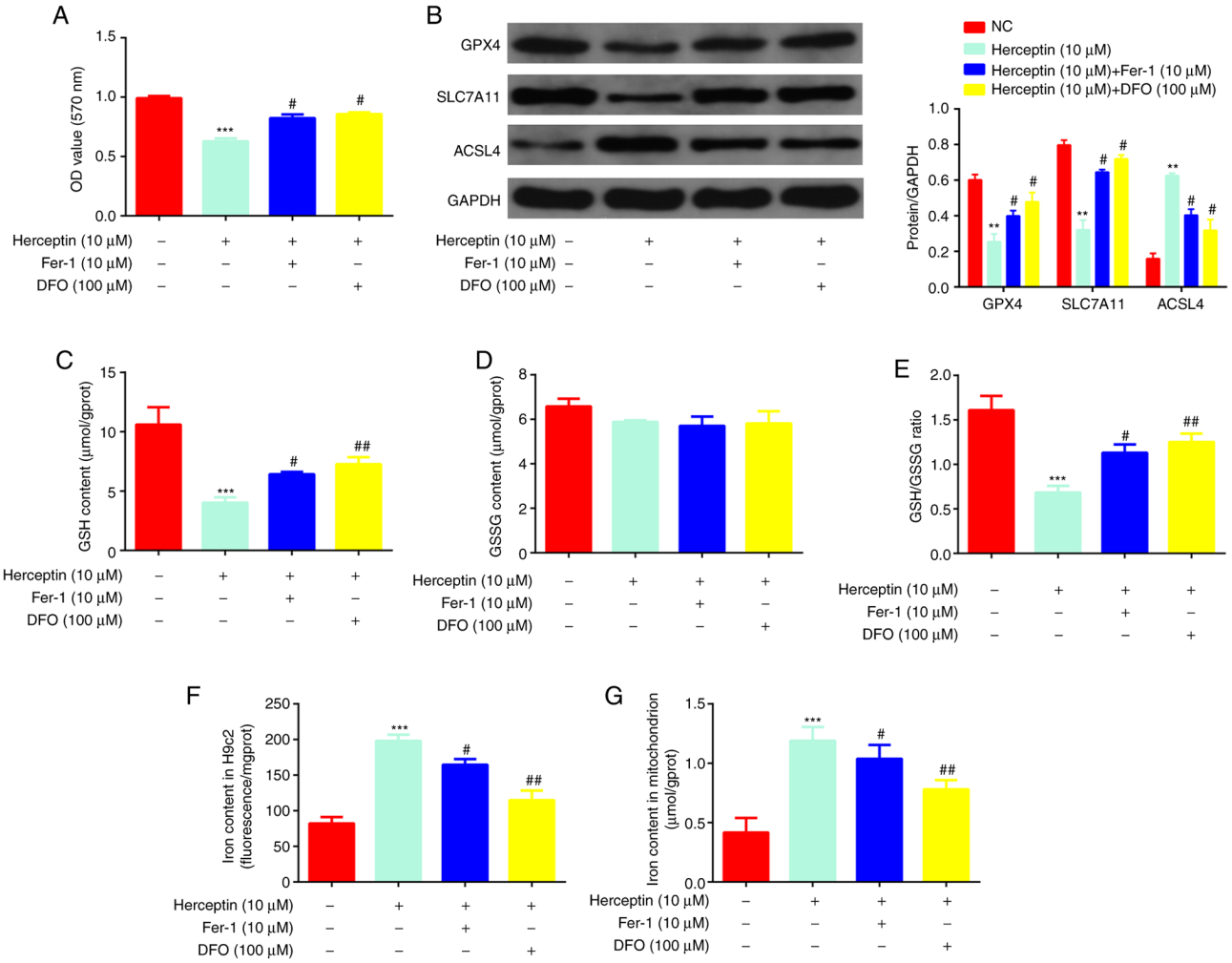

Figure 3. Fer-1 protects H9c2 cells against Herceptin-induced cell injury and ferroptosis. Fer-1 and DFO reversed the (A) Herceptin-induced reduction in cell viability, (B) Herceptin-induced decrease in GPX4 and SLC7A11 protein expression and Herceptin-induced increase in ACSL4 protein expression. Fer-1 and DFO reversed the Herceptin-induced (C) reduction in GSH content. (D) Fer-1 and DFO did not affect GSSG content. (E) Fer-1 and DFO reversed the Herceptin-induced reduction in the ratio of GSH/GSSG in H9c2 cells. Fer-1 and DFO reversed the Herceptin-induced increase in (F) intracellular and (G) mitochondrial iron levels in H9c2 cells. However, compared with DFO, the effects of Fer-1 were less potent. **P<0.01 and ***P<0.001 vs. NC. $^{\#}$P<0.05 and $^{\#\#}$P<0.01 vs. Herceptin (10 μM). Fer-1, ferrostatin-1; GPX4, glutathione peroxidase 4; SLC7A11, recombinant solute carrier family 7 member 11; ACSL4, acyl-CoA synthetase long chain family member 4; GSH, reduced glutathione; GSSG, oxidized glutathione; DFO, deferoxamine; OD, optical density.

cell cycle progression, breaking of DNA strands and/or cell death (28). In the present study, it was demonstrated that Herceptin reduced cell viability and increased both intracellular and mitochondrial ROS generation in H9c2 cells. This suggest that Herceptin induced cell injury and oxidative stress in H9c2 cells, which is consistent with a previous report that also showed the involvement of oxidative stress in Herceptin-mediated cardiotoxicity (29).

Ferroptosis is characterized by the iron-dependent accumulation of lipid peroxides to lethal levels (2). Excessive ROS accumulation can induce damage in numerous cell types, which is associated with decreased GSH content (30). GSH is a water-soluble tripeptide that consists of the amino acid triad of glutamine, cysteine and glycine, which exists in either the oxidized GSSG state or the reduced GSH state inside the cell (31). Therefore, it is crucial to sustain optimal GSH/GSSG ratios in the cells for survival (31). Mechanistically, GSH is a key antioxidant enzyme that participates in the clearance of ROS (32) and detoxification of various electrophilic compounds and peroxides by glutathione S-transferases and GPX through catalysis (31). In the present study, Herceptin was observed to decrease GPX4 expression and the GSH/GSSG ratio in H9c2 cells, suggesting that Herceptin induced ferroptosis in H9c2 cells, consistent with a previously published report that also demonstrated that ferroptosis may mediate Herceptin-induced cardiotoxicity (33).

Altered iron homeostasis results in excessive iron deposition in the heart, leading to progressive tissue damage (20). Excessive iron burden promotes oxidative stress, which serves an important role in the pathogenesis of iron overload-mediated heart disease (34), iron overload cardiomyopathy (18,35), myocardial injury and heart failure (36). However, to the best of our knowledge, the association between Herceptin-induced changes in iron homeostasis and ferroptosis in H9c2 cells has yet to be elucidated. GPX4 and SLC7A11 acts as ferroptosis inhibitors (37), GPX4 uses reduced glutathione to convert lipid hydroperoxides to lipid alcohols, thereby mitigating lipid peroxidation and inhibiting ferroptosis (38). The majority of cells obtain cysteine biologically through the import of extracellular cystine transporter SLC7A11 (39). ACSL4 is a lipid

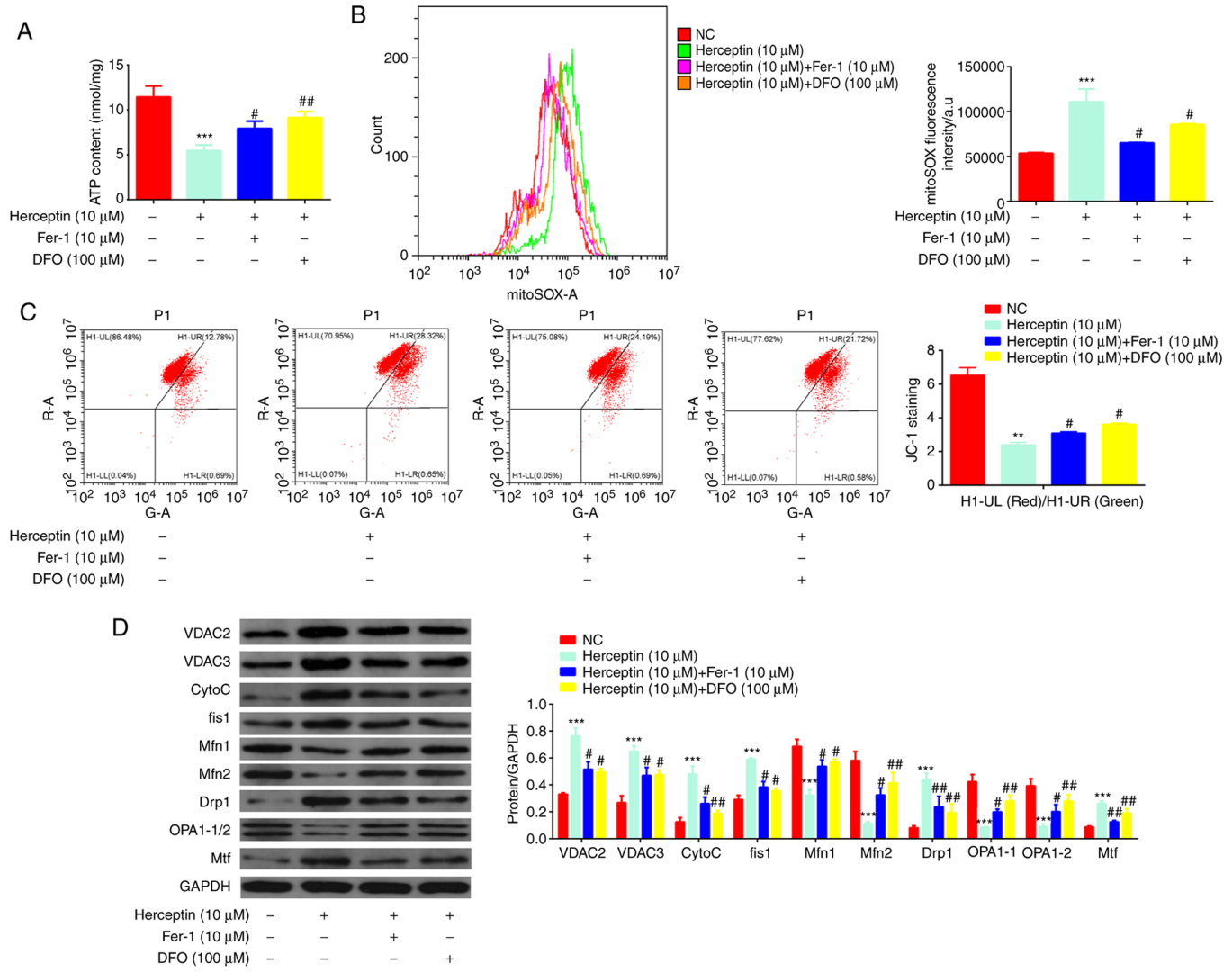

Figure 4. Fer-1 protects H9c2 cells from Herceptin-induced mitochondrial dysfunction. (A) Fer-1 and DFO reversed the Herceptin-induced reduction in ATP content. (B) Fer-1 and DFO reversed the Herceptin-induced increase in ROS levels. (C) Fer-1 and DFO reversed the Herceptin-induced decrease in mitochondrial membrane potential (UL, Red; UR, Green). (D) Fer-1 and DFO reversed the Herceptin-induced increase of Cyto *c*, VDAC2/3, fis1, Drp1 and Mtf expression, whilst also reversing the Herceptin-induced decrease in OPA1-1/2 and Mfn1/2 expression. However, compared with those by DFO, the effects of Fer-1 were less potent. **P<0.01 and ***P<0.001 vs. NC. $^{\#}$P<0.05 and $^{\#\#}$P<0.01 vs. Herceptin (10 μM). Fer-1, ferrostatin-1; ROS, reactive oxygen species; DFO, deferoxamine; Cyto *c*, cytochrome C; VDAC2/3, voltage-dependent anion-selective channels 2/3; fis1, mitochondrial fission 1 protein; Drp1, dynamin-related protein 1; OPA1-1/2, mitochondrial optic atrophy 1; Mfn1/2, Mitofusin 1/2; Mtf, mitochondrial ferritin.

metabolism enzyme required for ferroptosis and can elevate lipid peroxidation and ferroptosis (40). In detail, inactivation of GPX4 or SLC7A11 through genetic or pharmacological means has been previously found to induce ferroptosis (2). In addition, ferroptosis can be attenuated by the inactivation of ACSL4 (41). Therefore these aforementioned indicators of ferroptosis were detected in the present study. It was demonstrated that Fer-1 treatment reversed the Herceptin-induced reduction in H9c2 cell viability, reversed Herceptin-mediated decrease in GPX4 and SLC7A11 protein expression in addition to reversing the Herceptin-induced increase in ACSL4 protein expression. Furthermore, Fer-1 reversed the inhibitory effects of Herceptin on the GSH/GSSG ratio in H9c2 cells, as well as reversing the increase in intracellular and mitochondrial iron levels in H9c2 cells induced by Herceptin. These findings suggest that targeting ferroptosis can protect H9c2 cells from Herceptin-induced cardiomyocyte injury and ferroptosis.

Oxidative stress can also result in mitochondrial dysfunction (42). Since reductions in the mitochondrial membrane potential is associated with heart failure (43), the present study also assessed the effects of Fer-1 on Herceptin-induced mitochondrial dysfunction. Under physiological conditions, adult cardiac tissues primarily rely on fatty acid oxidation for the production of ATP, with ~70% ATP being generated by fatty acid metabolism (44). However, during heart failure, the overall production of ATP is decreased (45). The present study found that Fer-1 treatment restored mitochondrial membrane potential and ATP production, both of which were previously inhibited by Herceptin. In addition, Ferl-1 reversed the Herceptin-induced increases in ROS production. Subsequently, the expression levels of the associated proteins were also detected. Drp1 (fission gene, which increases mitochondrial division), Fis1 (fission gene, which increases mitochondrial division), Mfn1/2 (fusion gene, which increases mitochondrial fusion and mitochondrial connectivity)

and Opa1-1/2 (fusion gene, which increases mitochondrial fusion and mitochondrial connectivity) can regulate, maintain and remodel mammalian mitochondria dynamics and distribution (46). In addition, mitochondrial release of cytochrome *c* is a hallmark of cell death (47). ADP/ATP exchange is realized by VDAC2/3 on the outer mitochondrial membrane (48). Iron loss triggers mitophagy by induction of Mtf (49). It was observed that Fer-1 reversed the Herceptin-induced reduction in OPA1-1/2 and Mfn1/2 protein expression and Herceptin-induced increase in Cyto *c*, VDAC2/3, fis1, Drp1 and Mtf protein expression, suggesting that targeting ferroptosis protected H9c2 cells from Herceptin-induced mitochondrial dysfunction. However, compared with DFO, the effects of Fer-1 were not as potent effective.

Taken together, targeting ferroptosis can protect the cardiomyocytes from Herceptin-induced toxicity in the present H9c2 *in vitro* model. A previous study has shown that haploid embryonic stem cells have been used for toxicology drug screening (50), which may be useful for finding additional ferroptosis inhibitors to protect myocardial cells against chemotherapeutic drugs for cancer. The present study proposed that iron-dependent ferroptosis is one of the pathological processes underlying the development of Herceptin-induced cardiomyopathy. Mechanistically, Herceptin contributed to the release of free iron, which accumulated in the mitochondria. Furthermore, targeting ferroptosis also protected H9c2 cells from Herceptin-induced injury. Collectively, these findings provided novel insights into the pathogenic mechanisms underlying iron overload-induced cardiomyopathy and offer therapeutic targets for the development of novel strategies.

However, several limitations remain in the present study. There is a lack of *in vivo* evidence, rendering animal experiments a necessity for future study to verify the present findings, using techniques such as immunohistochemistry and echocardiography. Additionally, only ferroptosis was focused upon in the present study, such that other types of cell death, including apoptosis or autophagy, were not detected. Simultaneous observations of all four types of cell death should be detected in future investigations.

Acknowledgements

Not applicable.

Funding

The present study was funded by the Natural Science Foundation of Shaanxi Province (grant no. 2019JM-523) and the Fundamental Research Funds for the Central Universities (grant no. xzy012021059).

Availability of data and materials

The datasets used and/or analyzed during the current study are available from the corresponding author on reasonable request.

Authors' contributions

LS and QZ conceived the study, established the initial design of the study and confirmed the authenticity of all the raw data. LS, HW, SY, LZ and JJ performed the experiments and analyzed the data. QZ prepared the manuscript. All authors read and approved the final manuscript.

Ethics approval and consent to participate

Not applicable.

Patient consent for publication

Not applicable.

Competing interests

The authors declare that they have no competing interests.

References

1. Fuchs Y and Steller H: Programmed cell death in animal development and disease. Cell 147: 742-758, 2011.
2. Dixon SJ, Lemberg KM, Lamprecht MR, Skouta R, Zaitsev EM, Gleason CE, Patel DN, Bauer AJ, Cantley AM, Yang WS, *et al*: Ferroptosis: An iron-dependent form of nonapoptotic cell death. Cell 149: 1060-1072, 2012.
3. Angeli JPF, Shah R, Pratt DA and Conrad M: Ferroptosis inhibition: Mechanisms and opportunities. Trends Pharmacol Sci 38: 489-498, 2017.
4. Fang X, Wang H, Han D, Xie E, Yang X, Wei J, Gu S, Gao F, Zhu N, Yin X, *et al*: Ferroptosis as a target for protection against cardiomyopathy. Proc Natl Acad Sci USA 116: 2672-2680, 2019.
5. Linkermann A, Skouta R, Himmerkus N, Mulay SR, Dewitz C, De Zen F, Prokai A, Zuchtriegel G, Krombach F, Welz PS, *et al*: Synchronized renal tubular cell death involves ferroptosis. Proc Natl Acad Sci USA 111: 16836-16841, 2014.
6. Yang WS and Stockwell BR: Ferroptosis: Death by lipid peroxidation. Trends Cell Biol 26: 165-176, 2016.
7. Loibl S and Gianni L: HER2-positive breast cancer. Lancet 389: 2415-2429, 2017.
8. Slamon D, Eiermann W, Robert N, Pienkowski T, Martin M, Press M, Mackey J, Glaspy J, Chan A, Pawlicki M, *et al*: Adjuvant trastuzumab in HER2-positive breast cancer. N Engl J Med 365: 1273-1283, 2011.
9. Jerusalem G, Lancellotti P and Kim SB: HER2^{+} breast cancer treatment and cardiotoxicity: Monitoring and management. Breast Cancer Res Treat 177: 237-250, 2019.
10. Barish R, Gates E and Barac A: Trastuzumab-induced cardiomyopathy. Cardiol Clin 37: 407-418, 2019.
11. Whelan RS, Kaplinskiy V and Kitsis RN: Cell death in the pathogenesis of heart disease: Mechanisms and significance. Annu Rev Physiol 72: 19-44, 2010.
12. Pantopoulos K, Porwal SK, Tartakoff A and Devireddy L: Mechanisms of mammalian iron homeostasis. Biochemistry 51: 5705-5724, 2012.
13. Ward RJ, Zucca FA, Duyn JH, Crichton RR and Zecca L: The role of iron in brain ageing and neurodegenerative disorders. Lancet Neurol 13: 1045-1060, 2014.
14. Rouault TA: Iron metabolism in the CNS: Implications for neurodegenerative diseases. Nat Rev Neurosci 14: 551-564, 2013.
15. Reichert CO, de Freitas FA, Sampaio-Silva J, Rokita-Rosa L, Barros PL, Levy D and Bydlowski SP: Ferroptosis mechanisms involved in neurodegenerative diseases. Int J Mol Sci 21: 8765, 2020.
16. Torti SV and Torti FM: Iron and cancer: More ore to be mined. Nat Rev Cancer 13: 342-355, 2013.
17. Chen Y, Fan Z, Yang Y and Gu C: Iron metabolism and its contribution to cancer (Review). Int J Oncol 54: 1143-1154, 2019.
18. Lapice E, Masulli M and Vaccaro O: Iron deficiency and cardiovascular disease: An updated review of the evidence. Curr Atheroscler Rep 15: 358, 2013.
19. Kobayashi M, Suhara T, Baba Y, Kawasaki NK, Higa JK and Matsui T: Pathological roles of iron in cardiovascular disease. Curr Drug Targets 19: 1068-1076, 2018.
20. Wood JC: History and current impact of cardiac magnetic resonance imaging on the management of iron overload. Circulation 120: 1937-1939, 2009.

21. Valko M, Jomova K, Rhodes CJ, Kuča K and Musílek K: Redox- and non-redox-metal-induced formation of free radicals and their role in human disease. Arch Toxicol 90: 1-37, 2016.
22. Ichikawa Y, Ghanefar M, Bayeva M, Wu R, Khechaduri A, Naga Prasad SV, Mutharasan RK, Naik TJ and Ardehali H: Cardiotoxicity of doxorubicin is mediated through mitochondrial iron accumulation. J Clin Invest 124: 617-630, 2014.
23. Gujja P, Rosing DR, Tripodi DJ and Shizukuda Y: Iron overload cardiomyopathy: Better understanding of an increasing disorder. J Am Coll Cardiol 56: 1001-1012, 2010.
24. Kurokawa YK, Shang MR, Yin RT and George SC: Modeling trastuzumab-related cardiotoxicity in vitro using human stem cell-derived cardiomyocytes. Toxicol Lett 285: 74-80, 2018.
25. Baba Y, Higa JK, Shimada BK, Horiuchi KM, Suhara T, Kobayashi M, Woo JD, Aoyagi H, Marh KS, Kitaoka H and Matsui T: Protective effects of the mechanistic target of rapamycin against excess iron and ferroptosis in cardiomyocytes. Am J Physiol Heart Circ Physiol 314: H659-H668, 2018.
26. Wu C, Zhao W, Yu J, Li S, Lin L and Chen X: Induction of ferroptosis and mitochondrial dysfunction by oxidative stress in PC12 cells. Sci Rep 8: 574, 2018.
27. Xu T, Ding W, Ji X, Ao X, Liu Y, Yu W and Wang J: Oxidative stress in cell death and cardiovascular diseases. Oxid Med Cell Longev 2019: 9030563, 2019.
28. Chen S, Zhang Z, Qing T, Ren Z, Yu D, Couch L, Ning B, Mei N, Shi L, Tolleson WH and Guo L: Activation of the Nrf2 signaling pathway in usnic acid-induced toxicity in HepG2 cells. Arch Toxicol 91: 1293-1307, 2017.
29. Mohan N, Jiang J and Wu WJ: Implication of autophagy and oxidative stress in trastuzumab-mediated cardiac toxicities. Austin Pharmacol Pharm 2: 1005, 2017.
30. Lee H, Ki J, Lee SY, Park JH and Hwang GS: Processed panax ginseng, sun ginseng, decreases oxidative damage induced by tert-butyl hydroperoxide via regulation of antioxidant enzyme and anti-apoptotic molecules in HepG2 cells. J Ginseng Res 3: 248-255, 2012.
31. Anderson ME: Glutathione: An overview of biosynthesis and modulation. Chem Biol Interact 111-112: 1-14, 1998.
32. Townsend DM, Tew KD and Tapiero H: The importance of glutathione in human disease. Biomed Pharmacother 57: 145-155, 2003.
33. Ma W, Wei S, Zhang B and Li W: Molecular mechanisms of cardiomyocyte death in drug-induced cardiotoxicity. Front Cell Dev Biol 8: 434, 2020.
34. Oudit GY, Sun H, Trivieri MG, Koch SE, Dawood F, Ackerley C, Yazdanpanah M, Wilson GJ, Schwartz A, Liu PP and Backx PH: L-type $Ca2^{+}$ channels provide a major pathway for iron entry into cardiomyocytes in iron-overload cardiomyopathy. Nat Med 9: 1187-1194, 2003.
35. Pennell DJ, Udelson JE, Arai AE, Bozkurt B, Cohen AR, Galanello R, Hoffman TM, Kiernan MS, Lerakis S, Piga A, *et al*: Cardiovascular function and treatment in beta-thalassemia major: A consensus statement from the American heart association. Circulation 128: 281-308, 2013.
36. Munzel T, Gori T, Keaney JF Jr, Maack C and Daiber A: Pathophysiological role of oxidative stress in systolic and diastolic heart failure and its therapeutic implications. Eur Heart J 36: 2555-2564, 2015.
37. Lei G, Zhang Y, Koppula P, Liu X, Zhang J, Lin SH, Ajani JA, Xiao Q, Liao Z, Wang H and Gan B: The role of ferroptosis in ionizing radiation-induced cell death and tumor suppression. Cell Res 30: 146-162, 2020.
38. Seibt TM, Proneth B and Conrad M: Role of GPX4 in ferroptosis and its pharmacological implication. Free Radic Biol Med 133: 144-152, 2019.
39. Koppula P, Zhang Y, Zhuang L and Gan B: Amino acid transporter SLC7A11/xCT at the crossroads of regulating redox homeostasis and nutrient dependency of cancer. Cancer Commun (Lond.) 38: 12, 2018.
40. Cheng J, Fan YQ, Liu BH, Zhou H, Wang JM and Chen QX: ACSL4 suppresses glioma cells proliferation via activating ferroptosis. Oncol Rep 43: 147-158, 2020.
41. Yuan H, Li X, Zhang X, Kang R and Tang D: Identification of ACSL4 as a biomarker and contributor of ferroptosis. Biochem Biophys Res Commun 478: 1338-1343, 2016.
42. Aon MA, Bhatt N and Cortassa SC: Mitochondrial and cellular mechanisms for managing lipid excess. Front Physiol 5: 282, 2014.
43. Kadenbach B, Ramzan R, Moosdorf R and Vogt S: The role of mitochondrial membrane potential in ischemic heart failure. Mitochondrion 11: 700-706, 2011.
44. Opie LH: Metabolism of the heart in health and disease. I. Am Heart J 76: 685-698, 1968.
45. Ventura-Clapier R, Garnier A and Veksler V: Energy metabolism in heart failure. J Physiol 555: 1-13, 2004.
46. Chen H and Chan DC: Mitochondrial dynamics-fusion, fission, movement, and mitophagy-in neurodegenerative diseases. Hum Mol Genet 18: R169-R176, 2009.
47. Nguyen D, Alavi MV, Kim KY, Kang T, Scott RT, Noh YH, Lindsey JD, Wissinger B, Ellisman MH, Weinreb RN, *et al*: A new vicious cycle involving glutamate excitotoxicity, oxidative stress and mitochondrial dynamics. Cell Death Dis 2: e240, 2011.
48. Varikmaa M, Bagur R, Kaambre T, Grichine A, Timohhina N, Tepp K, Shevchuk I, Chekulayev V, Metsis M, Boucher F, *et al*: Role of mitochondria-cytoskeleton interactions in respiration regulation and mitochondrial organization in striated muscles. Biochim Biophys Acta 1837: 232-245, 2014.
49. Hara Y, Yanatori I, Tanaka A, Kishi F, Lemasters JJ, Nishina S, Sasaki K and Hino K: Iron loss triggers mitophagy through induction of mitochondrial ferritin. EMBO Rep 21: e50202, 2020.
50. Wang H, Zhang W, Yu J, Wu C, Gao Q, Li X, Li Y, Zhang J, Tian Y, Tan T, *et al*: Genetic screening and multipotency in rhesus monkey haploid neural progenitor cells. Development 145: dev160531, 2018.